

See discussions, stats, and author profiles for this publication at: <https://www.researchgate.net/publication/220003590>

Importance of Dynamics in Electron Excitation and Transfer of Organic Dyes

ARTICLE in THE JOURNAL OF PHYSICAL CHEMISTRY C · NOVEMBER 2010

Impact Factor: 4.77 · DOI: 10.1021/jp107032d

CITATIONS

8

READS

51

7 AUTHORS, INCLUDING:



Laura Walkup

Cincinnati Children's Hospital Medical Center

11 PUBLICATIONS 116 CITATIONS

SEE PROFILE



Krishanthi Weerasinghe

Southern Illinois University Carbondale

4 PUBLICATIONS 13 CITATIONS

SEE PROFILE



Xueqin Zhou

Tianjin University

24 PUBLICATIONS 112 CITATIONS

SEE PROFILE



Dongzhi Liu

Tianjin University

24 PUBLICATIONS 116 CITATIONS

SEE PROFILE

Importance of Dynamics in Electron Excitation and Transfer of Organic Dyes

Laura L. Walkup,[†] Krishanthi C. Weerasinghe,[†] Minli Tao,[‡] Xueqin Zhou,[§] Minhua Zhang,[‡] Dongzhi Liu,[§] and Lichang Wang^{*,†}

Department of Chemistry and Biochemistry, Southern Illinois University Carbondale, Carbondale, Illinois 62901, United States, R & D Center for Petrochemical Technology, Tianjin University, Tianjin 300072, China, and School of Chemical Engineering and Technology, Tianjin University, Tianjin 300072, China

Received: July 27, 2010; Revised Manuscript Received: September 14, 2010

Electron excitation and transfer of a triphenylamine derivative, triazine, anthraquinone, oxadiazole, triazine–anthraquinone, and triazine–oxadiazole were studied using density functional theory (DFT) and time-dependent DFT (TDDFT) calculations based on the B3LYP functional. The difference of the excitation wavelengths for anthraquinone using two basis sets, 6-311+G(d,p) and 6-31+G(d,p), was found to be within 4 nm. This indicates 6-31+G(d,p) can produce reasonable results and therefore is appropriate to use in calculations of large systems. The solvent effect on the electron excitation of these six molecules was investigated using three solvents: chloroform, dichloromethane, and ethanol. A red shift in excitation wavelength and enhanced absorption intensity were found in solution with respect to in vacuo condition. Furthermore, we introduced the concept of optically dynamic molecular orbitals (ODMOs) to account for the dynamic effect on electron transfer processes, which is critical in the interpretation of the results. A new dyad, consisting of the triphenylamine derivative–triazine–anthraquinone, is obtained to absorb triple photons of ~510, ~400, and ~320 nm. We predict this new dyad will be a good candidate for use in solar cells.

1. Introduction

Great progress has been made in developing organic solar cells since the early 1980s when only about 1% cell efficiency was achieved.¹ Dye-sensitized semiconductor solar cells (DSSCs),² denoted also as dye-sensitized solar cells (DSCs),³ have garnered much interest as a potentially low-cost energy alternative. In recent years, metal-free organic donor–acceptor dyes have attracted attention due to their lower cost and high molar absorption coefficients through intramolecular π – π^* transitions. Furthermore, a wide variety of structures can be designed more easily and economically and as more environmentally friendly replacements for ruthenium(II)–polypyridyl sensitizers in DSSCs.⁴ An impressive photovoltaic performance has been obtained using the metal-free organic dyes that showed efficiency up to 9.8%.⁵

Although remarkable advances have been made in the metal-free organic dyes as sensitizers for DSSCs, optimization of the chemical structures of existing dyes or development of new dyes is needed for further improvement on performance to match that of the ruthenium sensitizers which can achieve up to 11.2% cell efficiency.⁶ In general, an organic dye suitable for use in DSSCs consists of three moieties: a donor, a linker group, and an acceptor. Many experimental studies have been conducted implementing oligoenes, coumarins, triphenylamines, and porphyrins as donor moiety, carboxylic groups as acceptor moiety, and various structures with π -conjugation as the linker groups.⁴ We have synthesized and studied a series of porphyrin–linker–anthraquinone dyads by varying linker groups to explore the charge separation lifetime and found triazine is the best linker

group for this donor–acceptor system; the charge separation lifetime is 1.33 μ s for the porphyrin–triazine–anthraquinone dyad.⁷ This is encouraging as such a long lifetime of charge separation is an indicative of a candidate dye for potential solar cell applications. Triphenylamine-based dyes have been demonstrated to be good candidates for DSSCs.^{5,8} Triphenylamine shows a huge steric hindrance and can therefore prevent unfavorable dye aggregation at the semiconductor surface.⁹ We therefore attempt to combine a triphenylamine derivative as donor and our previously studied linker–acceptor, i.e., triazine–anthraquinone, to form dyads for DSSCs. Toward this, we focus on implementing density functional theory (DFT) and time-dependent DFT (TDDFT) methods to investigate the triphenylamine derivative, triazine, and anthraquinone as the potential moieties of dyes for DSSCs.

Computational studies have been widely used in the study of DSSCs.^{10,11} Great effort has been devoted to develop strategies and assess methods to allow accurate prediction of the electronic and spectroscopic properties of dyes.^{12,13} For UV–vis calculations, one of the most popular approaches remains TDDFT, which commonly provides accurate results for a reasonable computational effort, especially when hybrid functionals are used.^{9,12,14–18} The development and evaluations of TDDFT for calculating UV–vis spectra of dyes can be found in a themed issue of *Phys. Chem. Chem. Phys.*¹⁹ In this work, we also continued our efforts¹³ to develop computational strategies to study systems involving electron excitation and transfer processes. In particular, we focus on one of the open issues in the computational studies of acceptor–linker–donor systems: whether the data obtained for the isolated components can be used to predict the outcome of the whole covalently linked system. In our investigation of this issue on fluorescence sensors, it seems that the strategy works; however, in the sensor investigation, the linker group is not covalently bound to the

* To whom correspondence should be addressed. Tel.: (618)453-6476. E-mail: lwang@chem.siu.edu.

[†] Southern Illinois University Carbondale.

[‡] R & D Center for Petrochemical Technology, Tianjin University.

[§] School of Chemical Engineering and Technology, Tianjin University.

donor nor acceptor through π – π conjugations, and understandably the electrons are more localized versus the electrons of dyes for DSSCs.¹³

The HOMO (highest occupied molecular orbital) and LUMO (lowest unoccupied molecular orbital) energies are of obvious importance in the design of dyes for DSSCs and for photoinduced fluorescent sensors. In the work presented here, we found non-HOMO \rightarrow LUMO transitions, i.e., transitions taking place from an occupied orbital to a virtual orbital except for the HOMO to LUMO transition, are also involved in the electron excitation of the system. We refer to all the molecular orbitals that are involved in the electronic transitions as “optically active molecular orbitals (OAMOs)”. As such, the OAMOs are an extension of the HOMO/LUMO or “frontier orbitals”. As we will discuss here the involvement of multiple OAMOs in the electron excitation may be responsible for the efficiency of solar cells.

The molecular orbital energies obtained from DFT calculations are static. When electrons are excited to the virtual orbitals, the energy required is less than the difference between the calculated static energies of the OAMOs, as shown from the TDDFT calculations. This difference could be caused by changes in the energy levels of both involved orbitals. We would expect the energy of the fully occupied OAMO will rise slightly and that of the virtual OAMO will lower. In this work, we assume the difference is caused mostly by the lowering of virtual OAMO, and therefore, we introduce the concept of the “optically dynamic molecular orbital (ODMO)”, to replace the corresponding static virtual molecular orbital in the thermodynamics analysis. Indeed, the concept of ODMO is important in the design of organic dyes for solar cells, as the actual energy levels of the virtual molecular orbitals will be altered considerably due to this dynamic effect. As demonstrated in this work, using the concept of static OAMOs will not accurately describe the electron excitation and transfer process and in some cases may give a wrong prediction.

2. Computational Details

Six systems were considered, and their structures are shown in Figure 1: the donor triphenylamine modified with a phenylene linker group, abbreviated TPA; the linker triazine (TRI); the acceptors anthraquinone (AQ) and oxadiazole (OX); and the coupled linker–acceptor systems triazine–anthraquinone (TRI–AQ) and triazine–oxadiazole (TRI–OX). The latter two systems were selected as proofs-of-concept; both triazine–anthraquinone⁷ and triazine–oxadiazole²⁰ have been characterized experimentally as linker–acceptor systems in porphyrin-based dyes. Furthermore, the effect of solvent on the donor and acceptors was investigated; four solvent conditions were considered: in vacuo, chloroform, dichloromethane, and ethanol.

For each system in a given solvent environment, three types of calculations were carried out: geometry optimization, frequency calculation, and TDDFT calculation. All calculations were conducted in Gaussian03²¹ using the Becke’s three-parameter exchange functional with the Lee–Yang–Parr correlation functional (B3LYP)^{22–24} with a 6-311+G(d,p) basis set, except where noted otherwise. The solvent was treated using the polarized continuum model (PCM).²⁵ Full geometry optimizations were performed first without any constraints. The self-consistent field (SCF) convergence was 10^{-8} a.u.; the gradient and energy convergences were 10^{-4} and 10^{-5} a.u., respectively. Once the geometry optimization was performed, to ensure the optimized geometry (structure) was indeed an energetic minimum of the system, frequency calculations were

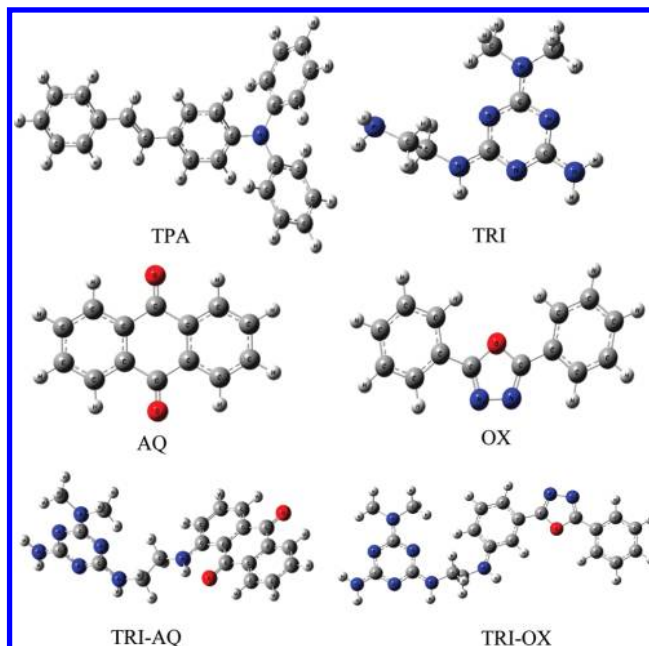


Figure 1. Structures of triphenylamine modified with a phenylene group (TPA), triazine (TRI), anthraquinone (AQ), oxadiazole (OX), triazine–anthraquinone (TRI–AQ), and triazine–oxadiazole (TRI–OX).

then conducted and inspected for imaginary frequencies. When the structure was confirmed to be at its minimum, i.e., there were no imaginary frequencies, TDDFT calculations using B3LYP were then performed to obtain information on the electron excitation. In the TDDFT calculations, six states were used to calculate excitation energies except for the cases of AQ and TRI–AQ systems where 12 states were used. The absorption spectra were obtained using GaussSum.²⁶

3. Results

3.1. Effect of Basis Set on the Absorption Spectra: Anthraquinone. Toward the development of a streamlined computational method, the effect of basis set choice on the calculated MO energies and the absorption spectrum of anthraquinone in gas phase was investigated. A smaller basis set would save computational time in similar future studies if the results using them are accurate. Additionally, how would optimization using a smaller basis set affect TDDFT results conducted using a larger basis set, and vice versa? Optimization and TDDFT calculations of gas-phase anthraquinone were carried out using the basis sets: both using the larger basis set 6-311+G(d,p); both using the smaller basis set 6-31+G(d,p); optimization using 6-311+G(d,p) followed by TDDFT using 6-31+G(d,p); and optimization using 6-31+G(d,p) followed by TDDFT using 6-311+G(d,p).

Table 1 summarized the excitation energies and other parameters obtained from TDDFT calculations. Three observations can be made from the data in Table 1. The first is that the excitation energy or wavelength was dependent on the basis set used in optimization calculations. A larger basis set, 6-311+G(d,p), gave an absorption wavelength of 323 nm, which is 3 nm shorter than that obtained using the smaller basis set, 6-31+G(d,p). The second observation is the oscillator strength dependent on the basis set in TDDFT calculations. A smaller basis set provided slightly larger oscillator strength. The third observation is the coefficient. Although the OAMOs are the same using both basis sets, the coefficients are dependent on

TABLE 1: Calculated Excitation Energies, Oscillator Strengths, and Molecular Orbitals (MOs) Involved in the Excitation for AQ Using Basis Sets 6-31+G(d,p) and 6-311+G(d,p)

basis sets ^a	energy (eV)	wavelength (nm)	oscillator strength	MOs	coefficient
6-31+G(d,p)/6-31+G(d,p)	3.81	326	0.1173	51 → 55 52 → 56	0.66621 0.18855
6-311+G(d,p)/6-311+G(d,p)	3.84	323	0.1113	51 → 55 52 → 56	0.66586 0.19277
6-31+G(d,p)/6-311+G(d,p)	3.80	326	0.1117	51 → 55 52 → 56	0.66573 0.19249
6-311+G(d,p)/6-31+G(d,p)	3.85	322	0.1169	51 → 55 52 → 56	0.66637 0.18876

^a Note: in the notation of basis sets, the first basis set was used for optimization and the second for TDDFT.

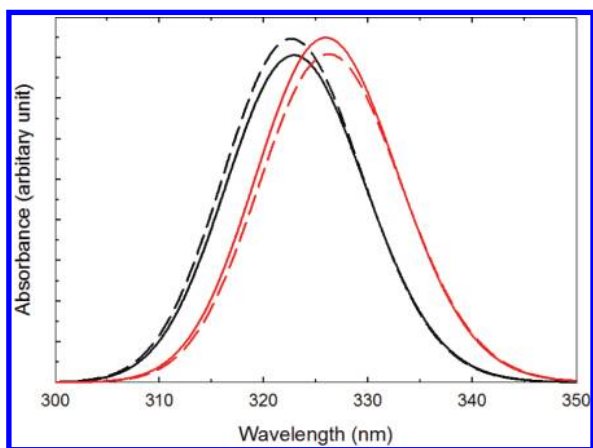


Figure 2. The UV-vis absorption spectra of AQ using different basis sets. The solid black, solid red, dashed black, and dashed red represent the results obtained using 6-311+G(d,p)/6-311+G(d,p), 6-31+G(d,p)/6-31+G(d,p), 6-311+G(d,p)/6-31+G(d,p), and 6-31+G(d,p)/6-311+G(d,p), respectively. The first basis set was used for the optimization and the second for the TDDFT calculation.

the basis set in TDDFT calculations. This dependence is the same as the oscillator strength.

Figure 2 depicts the simulated absorption spectra for these four conditions and makes the above observations more apparent. The solid red line is the result from using the smaller basis set 6-31+G(d,p) for both optimization and TDDFT while the dashed red line is from using the smaller basis set 6-31+G(d,p) for optimization and then the larger basis set 6-311+G(d,p) for TDDFT. Only the intensity of the transition differs between the two red lines; the wavelength remains the same at 326 nm. A similar trend is observed for the black lines. The solid black line represents using the larger basis set 6-311+G(d,p) for both calculations, and the dashed black line represents using first the larger basis set 6-311+G(d,p) for optimization and then conducting TDDFT in a smaller basis set 6-31+G(d,p). Again, the excitation occurs at the same wavelength, 322 nm; however, the two methods differ in the calculated intensity of the absorption peak. The calculated wavelength of the excitation is determined on the basis set chosen for the optimization.

We should mention that all the differences shown in the absorption wavelength/energy, oscillator strength, and coefficient are small. Therefore, we conclude that the use of a smaller basis set, 6-31+G(d,p), should be acceptable for the studies of large systems.

3.2. Effect of Solvent in UV-Vis Absorption Spectra: Triphenylamine Derivative, Anthraquinone, and Oxadiazole. Derivatives of triphenylamine are common donor moieties in organic dyes,^{4,5,27} and for the purposes of this investigation, we studied triphenylamine modified with a phenylene linker group,

TABLE 2: Calculated Excitation Energies, Oscillator Strengths, and Molecular Orbitals (MOs) Involved in the Excitation for TPA in Different Solvents Using B3LYP/6-31+G(d,p)

solvent	energy (eV)	wavelength (nm)	oscillator strength	MOs	coefficient
gas phase	3.17	391	0.4818	92 → 93	0.67051
	3.82	324	0.1761	92 → 95	0.67529
	4.17	298	0.1273	91 → 93	0.55222
				92 → 97	0.40675
chloroform	3.12	397	0.5946	92 → 93	0.67617
	3.78	328	0.2362	92 → 95	0.68130
	4.17	297	0.1273	91 → 93	0.52338
				92 → 97	0.44582
dichloromethane	3.09	401	0.5883	92 → 93	0.67617
	3.78	328	0.2330	92 → 95	0.68096
	4.13	300	0.1806	91 → 93	0.60017
				92 → 97	0.33089
ethanol	3.12	397	0.5740	92 → 93	0.67552
	3.79	327	0.2294	92 → 95	0.68032
	4.16	298	0.1435	91 → 93	0.54462
				92 → 97	0.41909

TABLE 3: Contours and Energies (eV) of the OAMOs of TPA in Different Solvents

Solvent	MO91	MO92 (HOMO)	MO93 (LUMO)	MO95	MO97
Gas Phase	-6.19	-5.16	-1.53	-0.75	-0.41
Chloroform	-6.17	-5.12	-1.48	-0.70	-0.38
Dichloromethane	-6.23	-5.19	-1.60	-0.78	-0.47
Ethanol	-6.19	-5.12	-1.51	-0.71	-0.39

abbreviated TPA. TPA has garnered attention for its high steric hindrance which limits dye aggregation,⁹ a common problem for DSSCs. Our computational studies of TPA were conducted using B3LYP/6-31+G(d,p). The TDDFT results relevant to the UV-vis absorption spectra are summarized in Table 2. As shown in Table 2, the optically active MOs include occupied MOs 91, 92 and virtual MOs 93, 95, 97. It is interesting to note that the excitations involve the same set of OAMOs in all the solvents. Additionally, one might suspect the contours of MOs not to vary in different solvents, and indeed the OAMOs share the same shape and nearly the same HOMO-LUMO gap among the solvents (Table 3).

In the simulated UV-vis absorption spectra (Figure 3), three excitations are present near 300, near 330, and near 400 nm; the latter excitation is the HOMO-LUMO transition, MO92 → MO93. The contours of these MOs in Table 3 show that this excitation also involves charge transfer. A red shift is observed as the polarity increases: the peak shifts from 391 nm in vacuo, to 397 nm in chloroform, and further to 401 nm in dichloromethane. However, in ethanol, the peak moves back to 397 nm, instead of red shifting further. In all solvents, chloroform,

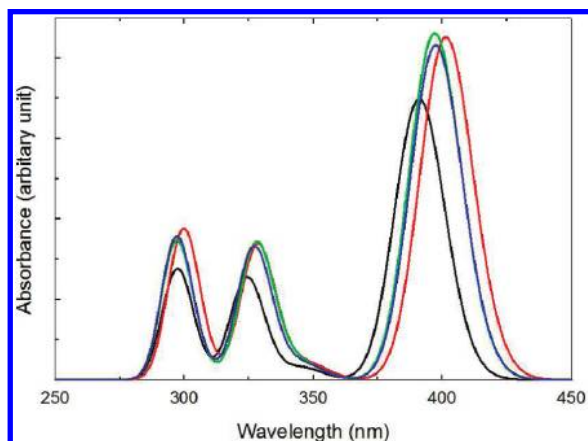


Figure 3. UV-vis absorption spectra of TPA. The black, green, red, and blue represent the B3LYP/6-31+G(d,p) results obtained in vacuo, CHCl_3 , CH_2Cl_2 , and EtOH, respectively.

TABLE 4: Calculated Excitation Energies, Oscillator Strengths, and Molecular Orbitals (MOs) Involved in the Excitation for AQ Using B3LYP/6-311+G(d,p)

solvent	energy (eV)	wavelength (nm)	oscillator strength	MOs	coefficient
gas phase	3.84	323	0.1111	51 \rightarrow 55	0.66562
				52 \rightarrow 56	0.19302
chloroform	3.71	334	0.1786	51 \rightarrow 55	0.67378
				53 \rightarrow 56	0.15922
dichloromethane	3.69	336	0.1776	51 \rightarrow 55	0.67328
				54 \rightarrow 56	0.16010
ethanol	3.68	337	0.1718	51 \rightarrow 55	0.67220
				52 \rightarrow 56	0.16360

dichloromethane, and ethanol, the absorption intensity is significantly increased.

TDDFT studies of AQ reveal the primary excitation to be not the HOMO (MO54) \rightarrow LUMO (MO55) transition. The data are summarized in Table 4. In vacuo, the transitions are MO51 \rightarrow MO55 and MO52 \rightarrow MO56 and the excitation wavelength is 323 nm. This wavelength red shifts to 334 nm, to 336 nm, and further to 337 nm as the solvent polarity increases from chloroform to dichloromethane and to ethanol, respectively. Furthermore, in addition to the MO51 \rightarrow MO55 transition, different OAMOs are involved in different solvents. For instance, the MO52 \rightarrow MO56 transition occurs in vacuo but MO53 \rightarrow MO56 in chloroform. This information is deceiving as a closer examination of the contours of these MOs (Table 5), MO52 in vacuo, and MO53 in chloroform, reveals the contours are the same even though these MOs are labeled differently in number. This illustrates that the relative energy of these MOs is altered due to solvent effects.

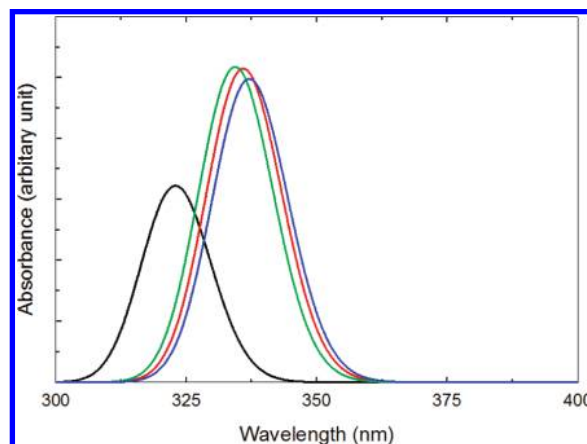








Figure 4. UV-vis absorption spectra of AQ. Black, green, red, and blue represent the B3LYP/6-311+G(d,p) results obtained in vacuo, CHCl_3 , CH_2Cl_2 , and EtOH, respectively.

Figure 4 shows the stacked simulated absorption spectra of AQ in different solvents. Like the TPA spectra, the absorption intensity of AQ is enhanced when solvent molecules are present. Additionally, the shapes of the OAMOs change with solvent. For instance, MO54, the HOMO, is more delocalized across the whole AQ molecule in both the gas phase and chloroform, but in dichloromethane, MO54 is isolated to the π -system of the rings. The LUMO (MO55) does not change appreciably; however it does slightly decrease in energy as the solvent polarity increases (Table 5). Table 5 also shows some “MO swapping” in solvents; for instance, MO52 in gas phase has the same shape as MO53 in both chloroform and ethanol and MO54 in dichloromethane. This MO contour denoted as B in Table 5, regardless of the solvent, is involved in the transition to the higher energy MO56, which plays into the excitation observed in the simulated absorption spectra.

Finally, we mention that our results agree with other calculations using B3LYP/6-31G^{28,29} and with the experiment (327 nm).³⁰ Because we are concerned with the absorption in the wavelengths longer than 300 nm, we did not plot the other two absorption bands of AQ at ~ 253 and ~ 286 nm.

Simulated absorption spectra of OX show three excitations (Figure 5). We shall focus our discussion on the primary excitation, MO58 \rightarrow MO59, which is a HOMO-LUMO transition. This transition red shifts from 303 to 310 nm as the solvent changes from gas phase to chloroform; in dichloromethane, the transition occurs at 309 nm. Furthermore, in ethanol, the most polar of the solvents considered, the excitation occurs at 308 nm. Therefore, the absorption wavelength decreases with the increase in solvent polarity, opposite of AQ.

TABLE 5: Energies and Contours of OAMOs of AQ in Different Solvents

Symbol	A	B	C	D	E	F
MO						
Orbital Energy (eV)						
Solvent	MO51	MO52	MO53	MO54 (HOMO)	MO55 (LUMO)	MO56
Gas Phase	A(-7.69)	B(-7.61)	C(-7.58)	D(-7.40)	E(-3.19)	F(-2.06)
Chloroform	A(-7.61)	C(-7.52)	B(-7.51)	D(-7.48)	E(-3.22)	F(-2.02)
Dichloromethane	A(-7.60)	C(-7.52)	D(-7.50)	B(-7.50)	E(-3.23)	F(-2.02)
Ethanol	A(-7.60)	C(-7.52)	B(-7.52)	D(-7.49)	E(-3.25)	F(-2.02)

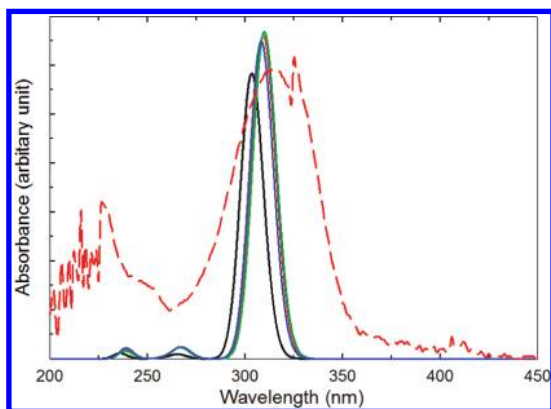


Figure 5. UV-vis absorption spectra of OX. Black, green, red, blue, and dashed lines represent the B3LYP/6-311+G(d,p) results obtained in vacuo, CHCl_3 , CH_2Cl_2 , EtOH, and the experimental data, respectively.

TABLE 6: Calculated Excitation Energies, Oscillator Strengths, and Molecular Orbitals (MOs) Involved in the Excitation for OX Using B3LYP/6-311+G(d,p)

solvent	energy (eV)	wavelength (nm)	oscillator strength	MOs	coefficient
gas	4.09	303	0.8056	58 \rightarrow 59	0.65890
chloroform	4.00	310	0.9233	58 \rightarrow 59	0.66873
dichloromethane	4.01	309	0.9139	58 \rightarrow 59	0.66865
ethanol	4.02	308	0.8957	58 \rightarrow 59	0.66799

TABLE 7: Contours and Energies of OAMOs of OX

Solvent	MO 58 (HOMO) (eV)	MO 59 (LUMO) (eV)
Gas Phase	-6.51	-2.02
Chloroform	-6.54	-2.02
Dichloromethane	-6.56	-2.03
Ethanol	-6.57	-2.04

The dashed line in the spectra is the experimental spectrum of OX in dichloromethane.²⁰ Our theoretical study shows good agreement with the experimental data.

The parameters obtained from the TDDFT calculations are summarized in Table 6. Again, the absorption intensity is increased in solvents with respect to in vacuo conditions. The contours of the HOMO and LUMO do not vary appreciably in different solvents, but the HOMO-LUMO gap increases from 4.49 eV in gas phase to 4.54 eV in dichloromethane and 4.53 eV in both chloroform and ethanol (Table 7).

3.3. Effect of Covalent Coupling on UV-Vis Absorption Spectra: Triazine-Anthraquinone and Triazine-Oxadiazole.

In a computational investigation of fluorescence sensors,¹³ we came to the conclusion that the energies and shapes of the OAMOs of the independent donor and acceptor moieties are not affected when the two are coupled covalently through the linker group. In the sensor study, the linker connects both the donor and acceptor moieties through single bonds. The electrons associated with the donor and acceptor moieties are not expected to be further delocalized due to the newly formed covalent bonds. However, it is not the case for dyes in DSSCs where forming π - π conjugation is the common feature of the linker groups. Therefore, we expect that the OAMOs, both in energy and shape, will be perturbed considerably and the predictions based solely on the results obtained from the isolated moieties will not accurately portray the energetics of the whole dye system. It is thus important to investigate how much perturbation the covalent coupling can cause. For the donor-

TABLE 8: Calculated Excitation Energies, Oscillator Strengths, and Molecular Orbitals (MOs) Involved in the Excitation for TRI-AQ and TRI-OX in Dichloromethane Using B3LYP/6-311+G(d,p)

system	energy (eV)	wavelength (nm)	oscillator strength	MOs	coefficient
TRI-AQ	2.42	512	0.1694	106 \rightarrow 107	0.65052
	3.78	328	0.1834	98 \rightarrow 107	0.37539
				99 \rightarrow 107	0.15715
				106 \rightarrow 108	0.53257
TRI-OX	3.19	389	0.0903	110 \rightarrow 111	0.68134
	4.05	306	0.8306	107 \rightarrow 111	0.22133
				108 \rightarrow 111	0.62480
				109 \rightarrow 111	0.11331

linker-acceptor systems TPA-TRI-AQ and TPA-TRI-OX, we chose to study the effect of coupling for TRI-AQ and TRI-OX only for the following reason. In the experimental work of porphyrin-TRI-AQ dyad,⁷ we showed that the UV-vis absorbance spectrum of the dyad in dichloromethane has a maximum at about 420 nm, which was essentially that of the isolated porphyrin. On the other hand, the absorption maximum for AQ at about 325 nm disappeared, and instead we found an excitation at about 250 nm. These observations imply the OAMOs of the porphyrin donor are not perturbed as much as those of AQ, the acceptor. Furthermore, our calculated absorption maximum (397 nm in ethanol shown in Table 2) for the isolated TPA is not very different from the absorption maximum (\sim 410 nm in methanol) of the TPA based dyes where conjugation was included.⁸ These lead us to focus on the covalent coupling effect in TRI-AQ and TRI-OX systems on the absorption spectra.

TDDFT results of the coupled systems TRI-AQ and TRI-OX in dichloromethane are summarized in Table 8 with the OAMOs illustrated in Figure 6. The TRI-AQ data in Table 8 show the excitation at 512 nm is a HOMO-LUMO transition (MO106 \rightarrow MO107). Compared to AQ, the presence of TRI raises the energy of the HOMO (MO106) in TRI-AQ to -6.00 eV from the HOMO (MO54) of AQ, which is -7.50 eV. Moreover, the contours of the TRI-AQ (Figure 6) show the HOMO electrons are not entirely delocalized in AQ but rather localized in the part close to TRI. The calculated HOMO energy of TRI is -6.22 eV, which is higher than the HOMO energy of AQ. Understandably, the HOMO energy of the TRI-AQ coupled system increases. The TRI-AQ LUMO is delocalized around the AQ moiety (Figure 6), but its shape has changed slightly with respect to the isolated AQ LUMO (E in Table 5). Also, the LUMO energy increases from -3.23 eV in AQ to -3.11 eV in TRI-AQ. We mention both MOs contain part of the TRI, with MO107 being more delocalized over the AQ moiety than MO106. Furthermore, this excitation (MO106 \rightarrow MO107) involves partial charge transfer from TRI to AQ and is not found in the AQ spectrum but was observed experimentally³⁰ and by other calculations.^{31,32}

Figure 7 depicts the spectra of TRI-AQ and AQ. In addition to the new absorption band at about 500 nm in TRI-AQ with similar absorption intensity as the original absorption band (red curve), the absorption band at 325 nm in TRI-AQ is blue-shifted with respect to the original band (red curve). The two bands in TRI-AQ indicate the TRI-AQ can absorb photons of different wavelengths to excite the electrons. This is advantageous in the application in DSSCs as long as the direction of electron transfer is desired.

For the TRI-OX system, there are two excitations (Table 8). The primary excitation occurs at 306 nm and is a non-

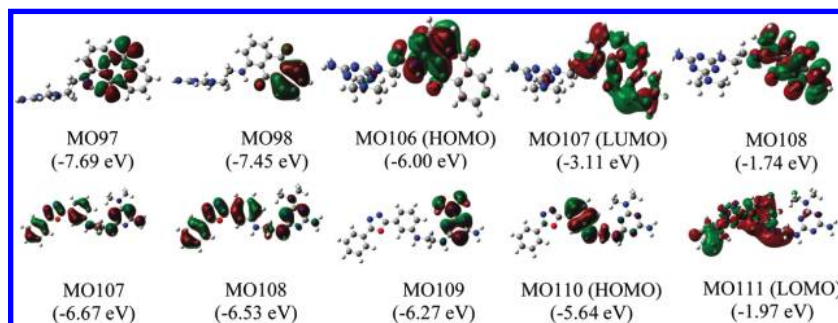


Figure 6. Contours of OAMOs and their corresponding energies for TRI–AQ (top) and TRI–OX (bottom) in dichloromethane obtained using B3LYP/6-311+G(d,p).

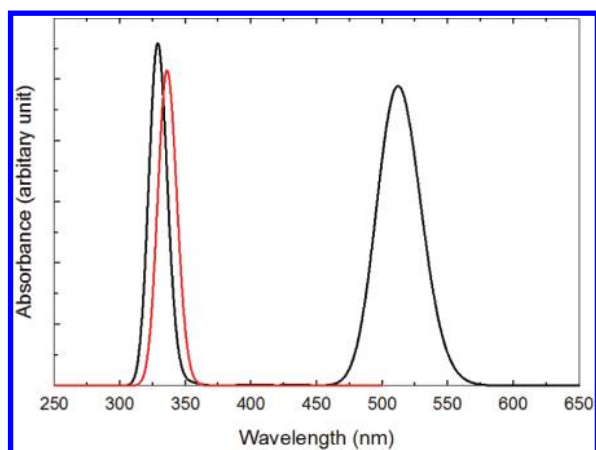


Figure 7. UV–vis spectra of TRI–AQ (black) and AQ (red) in dichloromethane obtained using B3LYP/6-311+G(d,p).

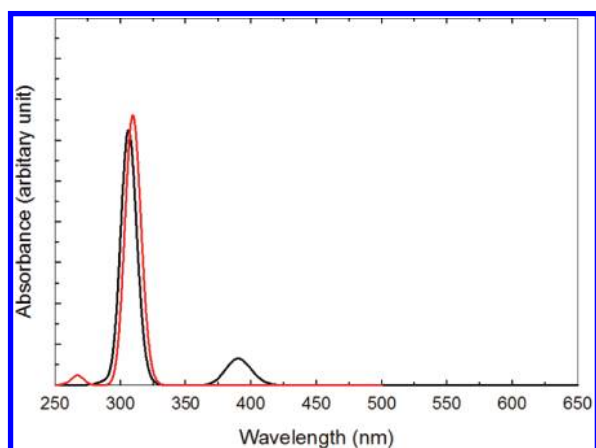


Figure 8. UV–vis spectra of TRI–OX (black) and OX (red) in dichloromethane obtained using B3LYP/6-311+G(d,p).

HOMO–LUMO transition. This absorption band is more corresponding to the primary absorption band of isolated OX, which is clearly shown in Figure 8. Furthermore, like the TRI–AQ vs AQ case, the main absorption band is blue-shifted. However, unlike the TRI–AQ vs AQ case, the newly formed absorption band in TRI–OX at about 390 nm is not comparable in intensity to the primary absorption band. Furthermore, the HOMO of TRI–OX (MO110 in Figure 6) is delocalized over both the middle of TRI and OX moieties. The HOMO and LUMO energies of TRI–OX are higher than the corresponding HOMO and LUMO energies of OX; thus the presence of TRI increased the HOMO and LUMO energies in the coupled system.

The difference between the isolated moiety and the corresponding covalently coupled system clearly shows the electron

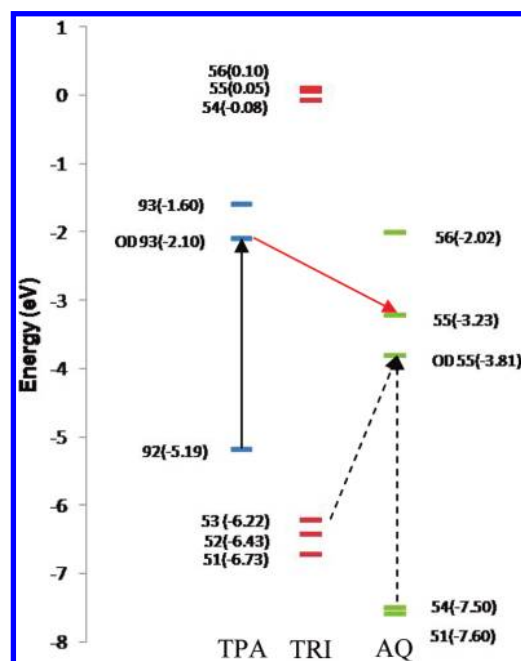


Figure 9. Molecular orbital energy diagram for the TPA–TRI–AQ dyad. The energies were calculated from the isolated moieties.

distribution of the entire system must be considered to make solid conclusion. This fact indicates that computational studies of dyes for DSSCs are more complicated than those in fluorescence sensor work due to the existence of π – π conjugation.

3.4. Optically Dynamic Molecular Orbitals: The Role of Dynamics and One Working Dyad TPA–TRI–AQ. On the basis of the encouraging results of the dyes including the triphenylamine derivatives⁵ and the long lifetime of charge separation exhibited by the linker triazine in the porphyrin–triazine–anthraquinone dyad,⁷ we constructed two dyads, TPA–TRI–AQ and TPA–TRI–OX. The TDDFT results on the energies of optically active molecular orbitals of these systems are summarized in Figure 9 for TPA–TRI–AQ dyad and in Figure 10 for TPA–TRI–OX dyad.

The thermodynamics of electron transfer processes involve a comparison of energy levels of OAMOs. For both dyads, upon absorption of a photon by TPA, the electrons will be excited to virtual orbital 93 (–1.60 eV), and then these excited electrons can be, in principle, transferred to the virtual orbitals 55 (–3.23 eV) and 56 (–2.02 eV) of AQ (Figure 9) or to 59 (–2.04 eV) of OX (Figure 10), because all of these OAMOs, i.e., 55 and 56 of AQ and 59 of OX, are lower in energy than orbital 93 of TPA. Therefore, on the basis of the above analysis, intramolecular electron transfer should take place in both dyads. We should mention that the coupling of TRI–AQ and TRI–OX

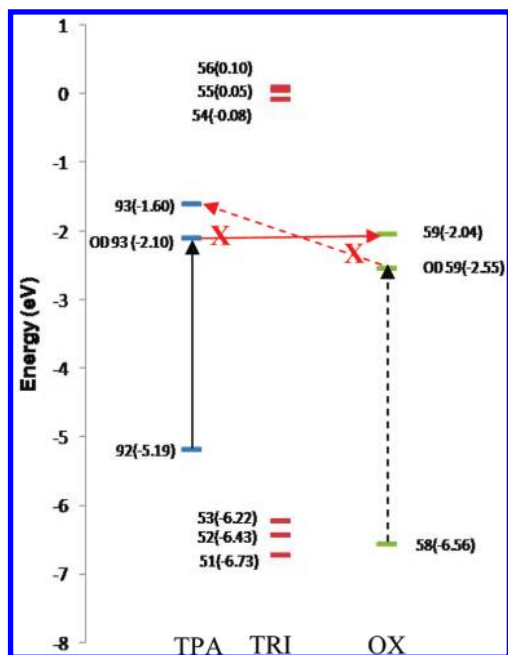


Figure 10. Molecular orbital energy diagram for the TPA-TRI-OX dyad. The energies were calculated from the isolated moieties.

does not affect the relative energies of these OAMOs associated with AQ and OX with respect to the orbital 93 of TPA.

However, the energy levels of these OAMOs discussed above are static. When the electrons are excited from orbital 92 to 93 of TPA, the actual energy required is 3.09 eV (Table 2), which is less than the difference between the static energies of orbitals 92 and 93 (3.59 eV). This 0.40 eV difference is mainly caused by the dynamics, i.e., the changes of both involved orbitals during excitation. The energy of the fully occupied orbital will rise slightly and that of the virtual orbital will lower. Here, we assume the energy reduction is caused only by lowering the energy of virtual orbital and defines a dynamically corrected virtual molecular orbital as the optically dynamic molecular orbital (ODMO) to replace the static virtual OAMO. In the case of TPA, we define the corresponding optically dynamic molecular orbital of 93 as ODMO93, labeled as OD93 in Figures 9 and 10, with energy of -2.10 eV, which was obtained by subtracting 0.40 eV from the static energy of orbital 93.

Employing the concept of ODMO, we reanalyzed the proposed two dyads. For TPA-TRI-AQ dyad, the electron transition from OD93 to orbital 56 of AQ will not occur as the energy of orbital 56 is higher than that of OD93 (Figure 9). Therefore, only the electron transfer from OD93 to orbital 55 is feasible. We note that orbital 55, not OD55, should be used in the analysis here as we do not expect this virtual orbital will change greatly during the electron transfer process. For TPA-TRI-OX dyad, the electrons excited to OD93 can no longer be transferred to OX (Figure 10), because orbital 59 has higher energy than OD93. This means the TPA-TRI-OX dyad cannot be a candidate for DSSCs as intramolecular electron transfer will not take place. It is clear from the above analysis on both systems, TPA-TRI-AQ and TPA-TRI-OX, the consideration of ODMOs is indeed important as the conclusion by applying the concept of ODMO differs from that without ODMO.

The TDDFT results shown in Figure 9 indicate that the new dyad, consisting of triphenylamine derivative-triazine-anthraquinone, can be potentially used as dye for DSSCs. More interestingly, the electrons from AQ moiety can be excited as

well by photons of different energies. The lower energy level of orbital 55 of AQ with respect to the virtual orbital 93 of TPA makes it impossible for intramolecular electron transfer from AQ to TPA, which is desired for DSSC application. Therefore, more electrons can be excited in the TPA-TRI-AQ dyad and directed toward semiconductors due to the triple photon excitations at ~ 510 , ~ 400 , and ~ 320 nm. Furthermore, on the basis of the experimental studies of porphyrin-TRI-AQ dyad,⁷ a long charge separation lifetime of about 1 μ s is expected for this proposed dyad.

4. Conclusions

The UV-vis absorption spectra for six systems, TPA, TRI, AQ, OX, TRI-AQ, and TRI-OX, were obtained from TDDFT calculations using B3LYP. A comparison of the UV-vis absorption spectra for anthraquinone using two basis sets, 6-311+G(d,p) and 6-31+G(d,p), indicates the 6-31+G(d,p) basis can be used in the calculations where a system is large. The TDDFT results clearly show the molecular orbitals involved in the electron excitation are not only the HOMO and LUMO. Therefore, one needs to consider the optically active molecular orbitals (OAMOs), defined as all the molecular orbitals involved in the excitation, in order to fully understand the efficiency of solar cells. In addition to in vacuo condition, the solvent effect on the excitation energy and absorption intensity was studied using three solvents: chloroform, dichloromethane, and ethanol. A red shift in excitation wavelength was found in solution with respect to in vacuo condition. Furthermore, the red shift generally increases with the solvent polarity. It is interesting to mention some MOs become active only in certain solvent conditions. In all cases, the presence of solvent increases the absorption intensity. When two molecules are covalently bound together, the UV-vis absorption spectra were affected by the coupling. Our results for the TRI-AQ and TRI-OX systems illustrated the active MOs are perturbed with respect to the respective isolated moieties due to the delocalization or relocation of electrons upon bonding. This fact makes the design of dyes for solar cells more challenging than that of fluorescence sensors; for dyes in DSSCs, the coupling of the moieties makes the electron distribution of the whole system no longer be a simple addition of the two electron distributions from isolated moieties.

It is important to include the dynamic effect in the consideration of electron transfer processes using the concept of the optically dynamic molecular orbitals (ODMOs). For both systems studied here, TPA-TRI-AQ and TPA-TRI-OX, the consideration of ODMOs is critical. In the TPA-TRI-OX system, we conclude that there will be no intramolecular electron transfer from TPA to OX when TPA absorbs a photon nor from OX to TPA when OX absorbs a photon. Without including the dynamics effect, one would conclude that the electron transfers from TPA to OX. A new dyad, consisted of TPA-TRI-AQ, is proposed on the basis of our calculations as a good candidate for DSSCs as it can absorb triple photons of ~ 510 , ~ 400 , and ~ 320 nm. On the basis of the experimental studies of a similar dyad, porphyrin-TRI-AQ,⁷ a long charge separation lifetime of about 1 μ s is expected for this proposed dyad.

Acknowledgment. This work is supported by ICCI (Grant 10/ER16).

References and Notes

- (1) Chamberlain, G. A. *Organic Solar Cells: A Review. Sol. Cells* **1983**, 8, 47-83.

- (2) Gratzel, M. Photoelectrochemical cells. *Nature* **2001**, *414*, 338–344.
- (3) Gratzel, M. Photovoltaic and Photoelectrochemical Conversion of Solar Energy. *Philos. Trans. R. Soc., A* **2007**, *365*, 993–1005.
- (4) Mishra, A.; Fischer, M. K. R.; Bauerle, P. Metal-Free Organic Dyes for Dye-Sensitized Solar Cells: From Structure:Property Relationships to Design Rules. *Angew. Chem., Int. Ed.* **2009**, *48*, 2474–2499.
- (5) Zhang, G.; Bala, H.; Cheng, Y.; Shi, D.; Lv, X.; Yu, Q.; Wang, P. High Efficiency and Stable Dye-Sensitized Solar Cells with an Organic Chromophore Featuring a Binary Π -Conjugated Spacer. *Chem. Commun. (Cambridge, U.K.)* **2009**, 2198–2200.
- (6) Nazeeruddin, M. K.; Angelis, F. D.; Fantacci, S.; Selloni, A.; Viscardi, G.; Liska, P.; Ito, S.; Takeru, B.; Gratzel, M. Combined Experimental and DFT-TDDFT Computational Study of Photoelectrochemical Cell Ruthenium Sensitizers. *J. Am. Chem. Soc.* **2005**, *127*, 16835–16847.
- (7) Tao, M.; Liu, L.; Liu, D.; Zhou, X. Photoinduced Energy and Electron Transfer in Porphyrin-Anthraquinone Dyad Bridged with a Triazine Group. *Dyes Pigm.* **2010**, *85*, 21–26.
- (8) Xu, W.; Peng, B.; Chen, J.; Liang, M.; Cai, F. New Triphenylamine-Based Dyes for Dye-Sensitized Solar Cells. *J. Phys. Chem. C* **2008**, *112*, 874–880.
- (9) Preat, J.; Michaux, C.; Jacquemin, D.; Perpete, E. A. Enhanced Efficiency of Organic Dye-Sensitized Solar Cells: Triphenylamine Derivatives. *J. Phys. Chem. C* **2009**, *113*, 16821–16833.
- (10) Duncan, W. R.; Prezhdo, O. V. Theoretical Studies of Photoinduced Electron Transfer in Dye-Sensitized TiO_2 . *Annu. Rev. Phys. Chem.* **2007**, *58*, 143–184.
- (11) Garavelli, M. Computational Organic Photochemistry: Strategy, Achievements and Perspectives. *Theor. Chem. Acc.* **2006**, *116*, 87–105.
- (12) Pastore, M.; Mosconi, E.; De Angelis, F.; Gratzel, M. A Computational Investigation of Organic Dyes for Dye-Sensitized Solar Cells: Benchmark, Strategies, and Open Issues. *J. Phys. Chem. C* **2010**, *114*, 7205–7212.
- (13) Hudson, G. A.; Cheng, L.; Yu, J.; Yan, Y.; Dyer, D. J.; McCarroll, M. E.; Wang, L. Computational Studies on Response and Binding Selectivity of Fluorescence Sensors. *J. Phys. Chem. B* **2010**, *114*, 870–876.
- (14) Park, S. S.; Won, Y. S.; Choi, Y. C.; Kim, J. H. Molecular Design of Organic Dyes with Double Electron Acceptor for Dye-Sensitized Solar Cell. *Energy Fuels* **2009**, *23*, 3732–3736.
- (15) Zhang, C. R.; Liu, Z. J.; Chen, Y. H.; Chen, H. S.; Wu, Y. Z.; Feng, W.; Wang, D. B. DFT and TD-DFT Study on Structure and Properties of Organic Dye Sensitizer TA-St-CA. *Curr. Appl. Phys.* **2010**, *10*, 77–83.
- (16) Badaeva, E. A.; Timofeeva, T. V. Role of Donor–Acceptor Strengths and Separation on the Two-Photon Absorption Response of Cytotoxic Dyes: A TD-DFT Study. *J. Phys. Chem. A* **2005**, *109*, 7276–7284.
- (17) Fantacci, S.; Amat, A.; Sgamellotti, A. Computational Chemistry Meets Cultural Heritage: Challenges and Perspectives. *Acc. Chem. Res.* **2010**, *43*, 802–813.
- (18) Tirado-Rives, J.; Jorgensen, W. L. Performance of B3LYP Density Functional Methods for a Large Set of Organic Molecules. *J. Chem. Theory Comput.* **2008**, *4*, 297–306.
- (19) Marques, M. A. L.; Rubio, A. Time-Dependent Density-Functional Theory. *Phys. Chem. Chem. Phys.* **2009**, *11* (22), 4421–4688.
- (20) Tao, M.; Liu, D.; Zhang, M.; Zhou, X. Photoinduced Energy and Electron Transfer in Porphyrin-Oxadiazole Dyads. *Acta Chim. Sin.* **2008**, *66*, 1252–1258.
- (21) Frisch, M. J.; Trucks, G. W.; Schlegel, H. N.; Scuseria, G. E.; Robb, M. A.; Cheeseman, J. R.; Montgomery, J. A. J.; Vreven, T.; Kudin, K. N.; Burant, J. C.; Millam, J. M.; Iyengar, S. S.; Tomasi, J.; Barone, V.; Mennucci, B.; Cossi, M.; Scalmani, G.; Rega, N.; Petersson, G. A.; Nakatsuji, H.; Hada, M.; Ehara, M.; Toyota, K.; Fukuda, R.; Hasegawa, J.; Ishida, M.; Nakajima, T.; Honda, Y.; Kitao, O.; Nakai, H.; Klene, M.; Li, X.; Knox, J. E.; Hratchian, H. P.; Cross, J. B.; Bakken, V.; Adamo, C.; Jaramillo, J.; Gomperts, R.; Stramann, R. E.; Yazyev, O.; Austin, A. J.; Cammi, R.; Pomelli, C.; Ochterski, J. W.; Ayala, P. Y.; Morokuma, K.; Voth, G. A.; Salvador, P.; Dannenberg, J. J.; Zakrzewski, V. G.; Dapprich, S.; Daniels, A. D.; Strain, M. C.; Farkas, O.; Malick, D. K.; Rabuck, A. G.; Clifford, S.; Cioslowski, J.; Stefanov, B. B.; Liu, G.; Liashenko, A.; Piskorz, P.; Komaromi, I.; Martin, R. L.; Fox, D. J.; Keith, T.; Al-Laham, M. A.; Peng, C. Y.; Nanayakkara, A.; Challacombe, M.; Grill, P. M. W.; Johnson, B.; Chen, W.; Wong, M.; W.; Gonzalez, C.; Pople, J. A. *Gaussian 03*, Revision B.05; Gaussian: Wallingford, CT, 2004.
- (22) Becke, A. D. Density-Functional Exchange-Energy Approximation with Correct Asymptotic Behavior. *Phys. Rev. A* **1988**, *38*, 3098–3100.
- (23) Becke, A. D. Density-Functional Thermochemistry. 3. The Role of Exact Exchange. **1993**, *98*, 5648–5652.
- (24) Lee, C.; Yang, W.; Parr, R. G. Development of the Colle-Salvetti Correlation-Energy Formula into a Functional of the Electron Density. *Phys. Rev. B* **1988**, *37*, 785–789.
- (25) Cancès, E.; Mennucci, B.; Tomasi, J. A New Integral Equation Formalism for the Polarizable Continuum Model: Theoretical Background and Applications to Isotropic and Anisotropic Dielectrics. *J. Chem. Phys.* **1997**, *107*, 3032–3041.
- (26) O’Boyle, N. M.; Tenderholt, A. L.; Langner, K. M. A Library for Package-Independent Computational Chemistry Algorithms. *J. Comput. Chem.* **2008**, *29*, 839–845.
- (27) Teng, C.; Yang, X.; Yang, C.; Li, S.; Cheng, M.; Hagfeldt, A.; Sun, L. Molecular Design of Anthracene-Bridged Metal-Free Organic Dyes for Efficient Dye-Sensitized Solar Cells. *J. Phys. Chem. C* **2010**, *114*, 9101–9110.
- (28) Guillaumont, D.; Nakamura, S. Calculation of the Absorption Wavelength of Dyes Using Time-Dependent Density-Functional Theory (TD-DFT). *Dyes Pigm.* **2000**, *46*, 85–92.
- (29) Perpete, E. A.; Wathelot, V.; Preat, J.; Lambert, C.; Jacquemin, D. Toward a Theoretical Quantitative Estimation of the λ_{max} of Anthraquinones-Based Dyes. *J. Chem. Theory Comput.* **2006**, *2*, 434–440.
- (30) Labhart, H. Zur quantitativen Beschreibung des Einflusses von Substituenten auf das Absorptionsspektrum ebener Molekeln. Anwendung auf. *Helv. Chim. Acta* **1957**, *40*, 1410–1420.
- (31) Fabian, J.; Nepras, M. Interpretation of the 9,10-Antraquinone Chromophore by Configuration Analysis. *Collect. Czech. Chem. Commun.* **1980**, *45*, 2605–2620.
- (32) Jacquemin, D.; Perpete, E. A.; Scuseria, G. E.; Ciofini, I.; Adamo, C. TD-DFT Performance for the Visible Absorption Spectra of Organic Dyes: Conventional versus Long-Range Hybrids. *J. Chem. Theory Comput.* **2008**, *4*, 123–135.